arXiv:hep-ph/9904257v3 1 Feb 2000

Is neutrino decay really ruled out as a solution to the atmospheric neutrino problem from Super-Kamiokande data?

Sandhya Choubey[a] *and Srubabati Goswami*[b]
[a] *Saha Institute of Nuclear Physics,*
1/AF, Bidhannagar, Calcutta 700064, INDIA.
[b] *Physical Research Laboratory, Ahmedabad 380009, INDIA*

Abstract

In this paper we do a detailed χ^2-analysis of the 848 days of Super-Kamiokande(SK) atmospheric neutrino data under the assumptions of $\nu_\mu - \nu_\tau$ oscillation and neutrino decay. For the latter we take the most general case of neutrinos with non-zero mixing and consider the possibilities of the unstable component in ν_μ decaying to a state with which it mixes (scenario (a)) and to a sterile state with which it does not mix (scenario (b)). In the first case Δm^2 (mass squared difference between the two mass states which mix) has to be $> 0.1\ eV^2$ from constraints on K decays while for the second case Δm^2 can be unconstrained. For case (a) Δm^2 does not enter the χ^2-analysis while in case (b) it enters the χ^2-analysis as an independent parameter. In scenario (a) there is Δm^2 averaged oscillation in addition to decay and this gets ruled out at 100.0% C.L. by the latest SK data. Scenario (b) on the other hand gives a reasonably good fit to the data for $\Delta m^2 \sim 0.001\ eV^2$.

PACS: 14.60.Pq
keywords: neutrinos; mixing; oscillations; decay

[a] e-mail: sandhya@tnp.saha.ernet.in
phone : 011-91-33-3375345
fax : 011-91-33-3374637
[b] e-mail: sruba@prl.ernet.in

1 Introduction

The recent data of Super-Kamiokande (SK) [1] have given a new impetus to the atmospheric neutrino problem and a possible interpretation in terms of neutrino oscillation. Moreover the high statistics of SK makes it possible to study the zenith-angle dependence of the neutrino flux from which one can conclude that the ν_μ's show signs of oscillation but the ν_e events are consistent with the no-oscillation hypothesis. Independently the results from the reactor experiment CHOOZ disfavours the $\nu_\mu - \nu_e$ oscillation hypothesis [2]. On the other hand large angle $\nu_\mu - \nu_\tau$ or $\nu_\mu - \nu_s$ (ν_s being a sterile neutrino) solution continues to give a good fit to the data. Nevertheless effort has been on to try out other possibilities to explain the anomaly observed in SK and one among these is neutrino decay [3, 4]. In [3] it was shown that neutrino decay gives a poor fit to the data. However they considered neutrinos with zero mixing. Barger *et al.* considered the situation of neutrino decay in the general case of neutrinos with non-zero mixing angle [4]. They showed that the neutrino decay fits the L/E distribution of the SK data well. The Δm^2 taken by them was $> 0.1\ eV^2$ so that the Δm^2 dependent term averages out. As pointed out in [4] such a constraint on Δm^2 is valid when the unstable state decays into some other state with which it mixes. If however the unstable state decays into a sterile state with which it does not mix then there is no reason to assume $\Delta m^2 > 0.1\ eV^2$.

In this paper we present our results of two-flavour $\nu_\mu - \nu_\tau$ oscillation and neutrino decay solutions to the atmospheric neutrino problem by doing χ^2-fit to the 848 days of sub-GeV and multi-GeV Super-Kamiokande data [5]. We have also presented the results of χ^2-fit to the 535 days SK data and have compared it with the results for the new data. For the neutrino decay analysis we take the most general case of neutrinos with non-zero mixing and consider two pictures

- $\Delta m^2 > 0.1\ eV^2$ (scenario (a))
- Δm^2 unconstrained (scenario (b))

We also explicitly demonstrate the behavior of the up-down asymmetry parameters [6, 7] in both scenarios.

Our analysis shows that scenario (a) is ruled out at 100%(99.99%) C.L. by the 848(535) days of SK data. However if we remove the constraint on Δm^2 and consider the possibility of decay into a sterile state then one can get an acceptable fit for $\Delta m^2 \sim 0.001 eV^2$ and $\sin^2 2\theta$ large.

The plan of the paper is as follows. In section 2 we present our results for two-generation $\nu_\mu - \nu_\tau$ oscillation analysis. In section 3.1 we present our results for the neutrino decay solution constraining Δm^2 to be $> 0.1 eV^2$. In section 3.2 we do a three parameter χ^2 analysis by removing the constraint on Δm^2. In section

4 we perform a comparative study of the three cases and indicate how one can distinguish experimentally between the scenario (b) and the $\nu_\mu - \nu_\tau$ oscillation case though both give almost identical zenith-angle distribution.

2 $\nu_\mu - \nu_\tau$ oscillation

In the two-flavour picture the probability that an initial ν_l of energy E remains a ν_l after traveling a distance L in vacuum is

$$P_{\nu_l\nu_l} = 1 - \sin^2 2\theta \sin^2(\pi L/\lambda_{osc}) \tag{1}$$

where θ is the mixing angle between the two neutrino states in vacuum and λ_{osc} is the oscillation wavelength defined as,

$$\lambda_{osc} = (2.5\ km)\ \frac{E}{GeV}\frac{eV^2}{\Delta m^2} \tag{2}$$

where Δm^2 denotes the mass squared difference between the two mass eigenstates. The expected number of l (e or μ) like 1 ring events recorded in the detector in presence of oscillations is given by

$$\begin{aligned} N_l &= n_T \int_0^\infty dE \int_{(E_l)_{\min}}^{(E_l)_{\max}} dE_l \int_{-1}^{+1} d\cos\psi \int_{-1}^{+1} d\cos\xi\ \frac{1}{2\pi}\int_0^{2\pi} d\phi \\ &\times \frac{d^2F_l(E,\xi)}{dE\ d\cos\xi} \cdot \frac{d^2\sigma_l(E,E_l,\cos\psi)}{dE_l\ d\cos\psi}\epsilon(E_l) \cdot\ P_{\nu_l\nu_l}(E,\xi). \end{aligned} \tag{3}$$

n_T denotes the number of target nucleons, E is the neutrino energy, E_l is the energy of the final charged lepton, ψ is the angle between the incoming neutrino ν_l and the scattered lepton l, ξ is the zenith angle of the neutrino and ϕ is the azimuthal angle corresponding to the incident neutrino direction (the azimuthal angle relative to the ψ has been integrated out). The zenith angle of the charged lepton is then given by

$$\cos\Theta = \cos\xi\cos\psi + \sin\xi\cos\phi\sin\psi \tag{4}$$

$d^2F_l/dEd\cos\xi$ is the differential flux of atmospheric neutrinos of type ν_l, $d^2\sigma_l/dE_l d\cos\psi$ is the differential cross section for $\nu_l N \to lX$ scattering and $\epsilon(E_l)$ is the detection efficiency for the 1 ring events in the detector. The efficiencies that were available to us are not the detection efficiencies of the charged leptons but some function which we call $\epsilon(E)$ defined as [8]

$$\epsilon(E) = \frac{\int \frac{d\sigma}{dE_l}\epsilon(E_l)dE_l}{\int \frac{d\sigma}{dE_l}dE_l} \tag{5}$$

$P_{\nu_l\nu_l}$ is the survival probability of a neutrino flavour l after traveling a distance L given by,

$$L = \sqrt{(R_e + h)^2 - {R_e}^2 \sin^2 \xi} - R_e \cos \xi \tag{6}$$

R_e being the radius of the earth and h is the height of the atmosphere where the neutrinos are produced. We use the atmospheric neutrino fluxes from [9]. For the sub-GeV events the dominant process is the charged current quasi-elastic scattering from free or bound nucleons. We use the cross-sections given in [10]. The events in multi-GeV range have contributions coming from quasi-elastic scattering, single pion production and multi pion production and we have used the cross-sections given in [11]. For the multi-GeV events we assume that the lepton direction Θ is the same as the incoming neutrino direction ξ. But actually they are slightly different. We simulate this difference in the zenith angles by smearing the angular distribution of the number of events with a Gaussian distribution having a one sigma width of 15^o for μ type events and 25^o for the e type events [12]. For the sub-GeV events, difference in direction between the charged lepton and the neutrinos are exactly taken care of according to eq. (3) and (4).

To reduce the uncertainty in the absolute flux values the atmospheric neutrino measurements are usually presented in terms of the double ratio

$$R = \frac{(\nu_\mu + \overline{\nu}_\mu)/(\nu_e + \overline{\nu}_e)_{\rm obsvd}}{(\nu_\mu + \overline{\nu}_\mu)/(\nu_e + \overline{\nu}_e)_{\rm MC}} \tag{7}$$

where MC denotes the Monte-Carlo simulated ratio. Different calculations agree to within better than 5% on the magnitude of this quantity. We use a similar quantity R, where

$$R \equiv \frac{(N_\mu/N_e)|_{osc}}{(N_\mu/N_e)|_{no-osc}}. \tag{8}$$

The quantities $N_{e,\mu}$ are the numbers of e-like and μ-like events, as per eq.(3). The numerator denotes numbers obtained from eq.(3), while the denominator the numbers expected with the survival probability as 1.

At the detector, the neutrino flux come from all directions. Thus, the total path length between the production point in the atmosphere and the detector varies from about 10 km to 13,000 km depending on the zenith angle. Neutrinos with zenith angle less than 90^o (*'downward neutrinos'*) travel a distance of $\sim$ 10 – 100 km from their production point in the atmosphere to the detector while the neutrinos with larger zenith angles (*'upward neutrinos'*) cross a distance of up to $\sim$ 13,000 km to reach the detector. Apart from altering the flavour-content of the atmospheric neutrino flux, oscillations could lead to the following effect: if the oscillation length is much longer than the height of the atmosphere but smaller than the diameter of the earth, only upward neutrinos coming from the opposite

side of the earth will have significant oscillations. These would show up as an up-down asymmetry in the event distribution. SK has enough statistics to study these up-down flux asymmetry. They divide the $(-1,+1)$ interval in $\cos\Theta$ in five equal bins: $(-1.0,-0.6)$, $(-0.6,-0.2)$, $(-0.2,+0.2)$, $(+0.2,+0.6)$, $(+0.6,+1.0)$ and give the number of events in each bin. The first two bins correspond to the upward neutrinos and the last two bins correspond to the downward neutrinos. To probe the up-down flux asymmetries we use the parameter Y defined in [7],

$$Y_l \equiv \frac{(N_l^{-0.2}/N_l^{+0.2})|_{osc}}{(N_l^{-0.2}/N_l^{+0.2})|_{no-osc}}. \tag{9}$$

Here $N_l^{-0.2}$ denotes the number of l-type events produced in the detector with zenith angle $\cos\Theta < -0.2$, *i.e.* the upward neutrino events while $N_l^{+0.2}$ denotes the number of l-type events for $\cos\Theta > 0.2$ *i.e.* events coming from downward neutrinos. The central bin has contributions from both upward and downward neutrinos and is not useful for studying the up-down asymmetry.

We minimize the χ^2 function defined as [7]

$$\chi^2 = \sum_i \left[\left(\frac{R^{exp} - R^{th}}{\delta R^{exp}} \right)^2 + \left(\frac{Y_\mu^{exp} - Y_\mu^{th}}{\delta Y_\mu^{exp}} \right)^2 + \left(\frac{Y_e^{exp} - Y_e^{th}}{\delta Y_e^{exp}} \right)^2 \right], \tag{10}$$

where the sum is over the sub-GeV and multi-GeV cases. The experimentally observed rates are denoted by the superscript "exp" and the theoretical predictions for the quantities are labeled by "th". ΔR^{exp} is the error in R obtained by combining the statistical and systematic errors in quadrature. ΔY^{exp} corresponds to the error in Y. For this we take only the statistical errors since these are much larger compared to the systematic errors. We include both the e-like and the μ-like up-down asymmetries in the fit so that we have 4 degrees of freedom (6 experimental data - 2 parameters) for the oscillation analysis in the two parameters Δm^2 and $\sin^2 2\theta$.

The use of these type of ratios for the χ^2 analysis test has been questioned in [13] because the error distribution of these ratios is non-Gaussian in nature. The alternative is to use the absolute number of e or μ type events taking into account the errors and their correlations properly [12, 14]. However as has been shown in [7] the use of the R's and Y's as defined above is justified within the 3σ region around the best-fit point for a high statistics experiment like SK and provides an alternative way of doing the χ^2-analysis. A comparison of the results of [7] with those obtained in [12, 14] shows that the best-fit points and the allowed regions obtained do not differ significantly in the two approaches of data fitting. The advantage of using the ratios is that they are relatively insensitive to the uncertainties in the neutrino fluxes and cross-sections as the overall normalization

factor gets canceled out in the ratio. We have included the Y_e in our analysis because to justify the $\nu_\mu - \nu_\tau$ oscillation scenario, it is necessary to check that χ^2 including the data on electron events gives a low value and hence it is the standard practice to include these in the χ^2-analysis [7, 12, 14]. The data that we have used are shown in Table 1 which corresponds to the 848 days [5] and the 535 days [15] of data.

Table 1: The SK data used in this analysis.

	848 days data		535 days data	
Quantity	$Sub-GeV$	$Multi-GeV$	$Sub-GeV$	$Multi-GeV$
R^{exp}	0.69	0.68	0.63	0.65
ΔR^{exp}	0.05	0.09	0.06	0.09
Y_μ^{exp}	0.74	0.53	0.76	0.55
ΔY_μ^{exp}	0.04	0.05	0.05	0.06
Y_e^{exp}	1.03	0.95	1.14	0.91
ΔY_e^{exp}	0.06	0.11	0.08	0.13

For the 2 flavour $\nu_\mu - \nu_\tau$ oscillation the χ^2_{min} that we get is 1.21 with the best-fit values as $\Delta m^2 = 0.003\ eV^2$ and $\sin^2 2\theta = 1.0$. This provides a good fit to the data being allowed at 87.64% C.L. If we use the 535 days data then the χ^2_{min} that we get is 4.25 with the best-fit values as $\Delta m^2 = 0.005\ eV^2$ and $\sin^2 2\theta = 1.0$, the g.o.f being 37.32%. Thus the fit becomes much better with the 848 days data with no significant change in the best-fit values. Though we have used a different procedure of data fitting, our results agree well with that obtained by the SK collaboration[1]. In fig. 1 we show the 90% C.L. ($\chi^2 \leq \chi^2_{min} + 4.61$) and the 99% C.L. ($\chi^2 \leq \chi^2_{min} + 9.21$) allowed region in the (Δm^2 , $\sin^2 2\theta$) plane for the $\nu_\mu - \nu_\tau$ oscillation hypothesis using the latest SK data.

3 Neutrino decay

The neutrino decay hypothesis assumes that there is an unstable component in ν_μ (say ν_2) which decays into one of the lighter states (say ν_3). Experimental considerations constrain ν_e to decouple from ν_2 and it's decay partners, so that

$$\nu_e \approx \nu_1 \tag{11}$$

$$\nu_\mu \approx \nu_2 \cos\theta + \nu_3 \sin\theta \tag{12}$$

[1]The best-fit values that the SK collaboration has got for the 848 days data are [5] $\Delta m^2 = 0.003$ eV^2, $\sin^2 2\theta = 0.995$ and $\chi^2/d.o.f = 55.4/67$. This corresponds to a g.o.f of 84.33%.

From (12) the survival probability of the ν_μ of energy E, with an unstable component ν_2, after traveling a distance L is given by,

$$\begin{aligned} P_{\nu_\mu\nu_\mu} &= \sin^4\theta + \cos^4\theta \exp(-4\pi L/\lambda_d) \\ &\quad + 2\sin^2\theta\cos^2\theta\exp(-2\pi L/\lambda_d)\cos(2\pi L/\lambda_{osc})\,, \end{aligned} \tag{13}$$

where λ_d is the decay length (analogous to the oscillation wavelength given by eq. (2)) defined as,

$$\lambda_d = 2.5km\frac{E}{GeV}\frac{eV^2}{\alpha} \tag{14}$$

and $\alpha = m_2/\tau_0$, m_2 being the mass of the state ν_2 and τ_0 the decay lifetime. The λ_{osc} appearing in eq. (13) is the wavelength of oscillations as defined in eq. (2) with $\Delta m^2 = m_2^2 - m_3^2$.

3.1 $\Delta m^2 > 0.1eV^2$

If the unstable component in the ν_μ state decays to some other state with which it mixes then bounds from K decays imply $\Delta m^2 > 0.1eV^2$ [16]. In this case the $\cos(2\pi L/\lambda_{osc})$ term averages to zero and the probability becomes

$$P_{\nu_\mu\nu_\mu} = \sin^4\theta + \cos^4\theta\exp(-4\pi L/\lambda_d)\,. \tag{15}$$

In figs. 2 and 3 we show the variation of R and Y with α for various values of $\sin^2\theta$ for the sub-GeV and multi-GeV cases. For higher values of α, the decay length λ_d given by eq. (14) is low and the exponential term in the survival probability is less implying that more number of neutrinos decay and hence R is low. As α decreases the decay length increases and the number of decaying neutrinos decreases, increasing R. For very low values of α the exponential term goes to 1, the neutrinos do not get the time to decay so that the probability becomes $1 - \frac{1}{2}\sin^2 2\theta$ and remains constant thereafter for all lower values of α. This is to be contrasted with the $\nu_\mu - \nu_\tau$ oscillation case where in the no oscillation limit the $\sin^2(\pi L/\lambda_{osc})$ term $\to 0$ and the survival probability $\to 1$. For multi-GeV neutrinos since the energy is higher the λ_d is higher and the no decay limit is reached for a larger value of α as compared to the sub-GeV case. This explains why the multi-GeV curves become flatter at a higher α. The behavior of the up-down asymmetry parameter is also completely different from the only oscillation case [17]. In particular the plateau obtained for a range of Δm^2 which was considered as a characteristic prediction for up-down asymmetries is missing here. For the decay case even for α as high as 0.001 eV^2, the decay length $\lambda_d = 2500\ (E/GeV)\ km$ so that the exponential term is 1, there is almost no decay for the downward neutrinos and the survival probability is $P = 1 - \frac{1}{2}\sin^2 2\theta$ while the upward going neutrinos have

some decay and so Y is less than 1. As α decreases, the λ_d increases, and the fraction of upward going neutrinos decaying decreases and this increases Y. For very small values of α even the upward neutrinos do not decay and $Y \to 1$ being independent of θ.

We also perform a χ^2 analysis of the data calculating the "th" quantities in (10) for this scenario. The best-fit values that we get are $\alpha = 0.33 \times 10^{-4}$ in eV^2 and $\sin^2\theta = 0.03$ with a $\chi^2_{\rm min}$ of 49.16. For 4 degrees of freedom this solution is ruled out at 100% C.L. The best-fit values for the 535 days of data that we get are $\alpha = 0.28 \times 10^{-4}$ in eV^2 and $\sin^2\theta = 0.08$ with a $\chi^2_{\rm min}$ of 31.71. For 4 degrees of freedom this solution is ruled out at 99.99% C.L. [18]. Thus the fit becomes worse with the 848 days data as compared to the 535 days data. We have marked the R and Y corresponding to the best-fit value of the parameters α and $\sin^2\theta$ in figs. 2 and 3. It can be seen that the best-fit value of R for the sub-GeV neutrinos is just below and that for the multi-GeV neutrinos is just above the $\pm 1\sigma$ allowed band of the SK 848 days of data. The up-down asymmetry parameter Y is quite low for the sub-GeV neutrinos and extremely high for the multi-GeV neutrinos as compared to that allowed by the data. The fig. 2 shows that for the sub-GeV neutrinos the data demands a lower value of α while from fig. 3 we see that the multi-GeV neutrinos need a much higher α to explain the SK data. It is not possible to get an α that can satisfy both the sub-GeV and the multi-GeV SK data, particularly it's zenith angle distribution. In this scenario, decay for the sub-GeV upward neutrinos is more than that for the multi-GeV upward neutrinos (downward neutrinos do not decay much) and as a result Y for sub-GeV is lower than the Y for multi-GeV, a fact not supported by the data. Since the 848 days data needs even lesser depletion of the sub-GeV flux as compared to the multi-GeV flux, the fit gets worse.

3.2 Δm^2 unconstrained

In this section we present the results of our χ^2-analysis removing the constraint on Δm^2. This case corresponds to the unstable neutrino state decaying to some sterile state with which it does not mix [4]. The probability will be still given by eq. (13).

In fig. 4 and 5 we plot the R vs. Δm^2 and Y vs. Δm^2 for the sub-GeV and multi-GeV data for $\alpha = 0.3 \times 10^{-5} eV^2$ (which is the best-fit value we get for the 848 days data) and compare with the curve obtained for the best-fit value of $\sin^2\theta$ (=0.5) for the only oscillation case (solid line). For the best-fit value of α that we get, the downward neutrinos do not have time to decay while the upward neutrinos undergo very little decay. Thus the curves are very similar in nature to the only oscillation curves. In the sub-GeV case (fig. 4), for high values of Δm^2 around

0.1 eV^2 both upward and downward neutrinos undergo Δm^2 independent average oscillations and R stays more or less constant with Δm^2 . For the upward going neutrinos in addition to average oscillation there is little amount of decay as well and hence Y $\sim N_{up}/N_{down}$ is $\lesssim 1$. As Δm^2 decreases to about 0.05 eV^2 the oscillation wavelength increases – for upward neutrinos it is still average oscillation but for the downward neutrinos, the $\cos(2\pi L/\lambda_{osc})$ term becomes negative which corresponds to maximum oscillation effect and the survival probability of these neutrinos decreases, and hence R decreases; while the upward neutrinos continue to decay and oscillate at the same rate and Y becomes greater than 1. As Δm^2 decreases further, the downward neutrino oscillation wavelength becomes greater than the distance traversed and they are converted less and less and thus R increases and Y decreases. Below $\Delta m^2 = 0.001$ eV^2 the downward neutrinos stop oscillating completely while for the upward neutrinos the $\cos(2\pi L/\lambda_{osc})$ term goes to 1, and R and Y no longer vary with Δm^2 .

For the multi-GeV case (fig. 5) the oscillation wavelength is more than the sub-GeV case and for Δm^2 around 0.1 eV^2 the $\cos(2\pi L/\lambda_{osc})$ term stays close to 1 for the downward neutrinos; while the upward neutrinos undergo average oscillations and slight decay and Y is less than 1. As Δm^2 decreases the downward neutrinos oscillate even less and the upward neutrinos also start departing from average oscillations and hence R increases and Y decreases. Around 0.01 eV^2 the downward neutrinos stop oscillation while for upward neutrinos the oscillation effect is maximum ($\lambda \sim L/2$) and the $cos(2\pi L/\lambda_{osc})$ term is $\sim$ -1 and Y stays constant with Δm^2 . As Δm^2 decreases further the upward neutrino oscillation wavelength increases and they oscillate less in number making both R and Y approach 1 for Δm^2 around 0.0001 eV^2. For multi-GeV neutrinos the decay term contributes even less as compared to the sub-GeV case.

We perform a χ^2 minimization in the three parameters Δm^2 , $\sin^2 2\theta$ and α. The best-fit values that we get are $\Delta m^2 = 0.003eV^2$, $\sin^2 2\theta = 1.0$ and $\alpha = 0.3 \times 10^{-5} eV^2$. The χ^2 minimum that we get is 1.11 which is an acceptable fit being allowed at 77.46% C.L.. For the 535 days data the best-fit values that we get are $\Delta m^2 = 0.002eV^2$, $\sin^2 2\theta = 0.87$ and $\alpha = 0.0023eV^2$ with a $\chi^2_{\rm min}$ of 4.14 which is allowed at 24.67% C.L.. Thus compared to the 535 days data, the fit improves immensely and the best-fit shifts towards the oscillation limit, the best-fit value of the decay constant α being much lower now. It is to be noted however, that the best-fit in this model does not come out to be $\alpha = 0.0$, *viz* the only oscillation limit. In table 2 we give the contributions to χ^2 from the R's and Y's at the best-fit value of α and for the $\alpha = 0.0$ case.

Table 2: The various contributions to the ${\chi^2}_{\rm min}$ at the best-fit value of α and at α=0.0

Quantity	$\alpha = 0.3 \times 10^{-5}$ eV^2	$\alpha = 0.0$ eV^2
R^{sg}	0.085	0.021
Y_μ^{sg}	0.011	0.033
R^{mg}	0.48	0.56
Y_μ^{mg}	0.014	0.073
Y_e^{sg}	0.344	0.344
Y_e^{mg}	0.176	0.176

Thus from the contributions to χ^2 we see that for the best- fit case there is improvement for the multi-GeV R and Y as compared to the $\alpha = 0.0$ case. The χ^2 for sub-GeV Y also improves. In fig. 6 we plot the $\chi^2 - \chi^2_{\rm min}$ vs. α with Δm^2 and $\sin^2 2\theta$ unconstrained. There are two distinct minima in this curve – one for lower values and another at higher values of α. The best-fit Δm^2 in both cases is ~ 0.001 eV^2. In this model there are two competing processes – oscillation and decay. For lower values of α the decay length is greater than the the oscillation wavelength and oscillation dominates. The decay term $\exp(-\alpha L/E)$ is close to 1 and does not vary much with the zenith distance L. As α increases the exponential term starts varying very sharply with L and the variation is much more sharp for the sub-GeV as compared to multi-GeV. This behavior is inconsistent with the data and that is why one gets a peak in $\Delta\chi^2$ for higher α. As α increases further the $\exp(-\alpha L/E)$ term goes to zero for the upward neutrinos and there is complete decay of these neutrinos while the downward neutrinos do not decay, the exponential term still being 1. Whenever the exponential term is 0 or 1 for the upward neutrinos, the wrong energy dependence of this term does not spoil the fit and these scenarios can give good fit to the data. Even though fig. 6 shows that the data allows a wide range of α, we get the two distinct minima in the $\Delta\chi^2$ vs. α curve for high and low α values, for both the 535 days (dotted line) and 848 days (solid line) data. But while the 848 days data prefers the lower α limit, the 535 days data gives a better fit for the high α limit. The reason behind this is that for the 848 days data the R is much higher than for the 535 days data. Hence the 848 days data prefers lower α and hence lower suppression.

In fig. 7 we show the 90% and 99% C.L. allowed parameter region in the Δm^2 - $\sin^2 2\theta$ plane for a range of values of the parameter α. In fig. 8 we show the 90% and 99% C.L. contours in the α - $\sin^2 2\theta$ plane fixing Δm^2 at different values. These contours are obtained from the definition $\chi^2 \leq \chi^2{}_{\rm min} + \Delta\chi^2$, with $\Delta\chi^2 =$ 6.25 and 15.5 for the three parameter case for 90% and 99% C.L. respectively. The bottom left panel in fig 7 is for the best-fit value of α. For high α (the top left panel) no lower limit is obtained on Δm^2, because even if Δm^2 becomes so low so that there is no oscillation the complete decay of upward neutrinos can explain

their depletion. As we decrease α the allowed parameter region shrinks and finally for $\alpha = 0$ we get the two parameter limit modulo the small difference in the C.L. definitions for the two and three parameter cases. The upper right panel of fig. 8 corresponds to the best-fit value of Δm^2 . For very low α, even though there is no decay, we still have oscillations and that ensures that when Δm^2 is large enough there is no lower bound on α as evident in the fig. 8. For $\Delta m^2 = 10^{-4} eV^2$ the neutrinos stop oscillating and hence we get a lower bound on α beyond which the depletion in the neutrino flux is not enough to explain the data.

4 Comparison and Conclusion

In fig. 9 we show the histogram of the muon event distributions for the sub-GeV and multi-GeV data under the assumptions of $\nu_\mu - \nu_\tau$ oscillation, and the two scenarios of neutrino decay for the best-fit values of the parameters both for the 535 and the 848 days of data. From the figs. it is clearly seen that the scenario (a) (big dotted line) ($\Delta m^2 \ > 0.1 eV^2$) does not fit the data well there being too much suppression for the sub-GeV upward going neutrinos and too less suppression for the multi-GeV upward going neutrinos. The scenario (b) (Δm^2 unconstrained, small dashed line), however, reproduces the event distributions well. However with the 848 days data the sub-GeV events are reproduced better as compared to the 535 days data and the quality of the fit improves.

The neutrino decay is an interesting idea as it can preferentially suppress the upward ν_μ flux and can cause some up-down asymmetry in the atmospheric neutrino data. However the intrinsic defect in the decay term $\exp(-\alpha L/E)$ is that one has more decay for lower energy neutrinos than for the higher energy ones. Thus neutrino decay by itself fails to reproduce the observed data [3]. If however one considers the most general case of neutrinos with non-zero mixing then there are three factors which control the situation

- the decay constant α which determines the decay rate
- the mixing angle θ which determines the proportion of neutrinos decaying and mixing with the other flavour
- the Δm^2 which determines if there are oscillations as well

If the heavier state decays to a state with which it mixes then Δm^2 has to be $> 0.1 eV^2$ because of bounds coming from K decays [16]. The best-fit value of α that one gets is $0.33 \times 10^{-4} eV^2$ with the latest SK data. At this value of α the $e^{-\alpha L/E}$ term tends to 1 for the downward going neutrinos signifying that they do not decay much. The survival probability goes to $(1 - \frac{1}{2}\sin^2 2\theta)$ which is just the

average oscillation probability. In order to suppress this average oscillation the best-fit value of $\sin^2\theta$ comes out to be small in this picture. For the upward going neutrinos, in scenario (a), there will be both decay and average oscillations. If one had only average oscillation then the probability would have stayed constant for a fixed value of the mixing angle θ. But because of the exponential decay term the survival probability drops very sharply as we go towards $\cos\Theta$=-1.0. The drop and hence the decay is more for lower energy neutrinos. As a result the sub-GeV flux gets more depleted than the multi-GeV flux, a fact not supported by the data. In fact the 848 days data requires the sub-GeV flux to be even less suppressed than the multi-GeV flux as compared to the 535 days data and the fit worsens with the 848 days data. The small mixing signifies that the ν_μ has a large fraction of the unstable component ν_2 (see eq. (12)). Hence the constant α comes out to be low so that the decay rate is less to compensate this. However even at the best-fit α of 0.33 $\times 10^{-4} eV^2$ the survival probability in the bin with $\cos\Theta$ between -1.0 to -0.6 comes out to be 0.15 for E=1 GeV, much lower than the value of ~ 0.5 as required by the data. Thus scenario (a) fails to explain the upward going neutrino data properly because of two main reasons

- θ is low in order to suppress the average oscillations of the downward neutrinos
- the energy dependence of the exponential decay term is in conflict with the data

In the scenario (b), in addition to mixing with ν_τ, the unstable component in ν_μ decays to some sterile state with which it does not mix. In this case there is no restriction on Δm^2 and it enters the χ^2 fit as an independent parameter. We find that

- The best-fit Δm^2 does not come out naturally to be in the Δm^2 independent average oscillation regime of $> 0.1\ eV^2$, rather it is $0.003 eV^2$.
- The best-fit value of the decay constant $\alpha = 0.3 \times 10^{-5} eV^2$ implying that the decay rate is small so that the mixing angle is maximal ($\sin^2\theta = 0.5$).
- Large values of α giving complete decay of upward neutrinos are also allowed with a high C.L. In fact with 535 days data the best-fit was in this region.
- The best-fit value of the decay constant α is non-zero signifying that a little amount of decay combined with Δm^2 dependent oscillations gives a better fit to the data.

At the best-fit values of the parameters there is no oscillation of the downward neutrinos so that the $\cos(2\pi L/\lambda_{osc})$ term goes to 1. The decay term also goes to 1 signifying that there is not much decay either for the downward neutrinos and the survival probability is ≈ 1 without requiring the mixing angle to be low. On the other hand for the upward neutrinos there are oscillations as well as little amount of decay. The sub-GeV upward neutrinos have smaller oscillation wavelength and they are close to the average oscillation limit (survival probability ~ 0.5) while for the multi-GeV neutrinos the oscillation wavelength is such that one has maximum oscillations and the survival probability is less than 0.5. Thus this scenario reproduces the correct energy dependence of the suppression – namely sub-GeV is suppressed less as compared to multi-GeV neutrinos. The best-fit value of α being even smaller now than the scenario (a) the decay term $e^{-\alpha L/E}$ does not vary very sharply with the zenith distance L or the energy E so that its wrong energy dependence does not spoil the fit.

The conversion probability of ν_μ to ν_τ is given by

$$P_{\nu_\mu\nu_\tau} = \frac{1}{4}\sin^2 2\theta\{1 + \exp(-4\pi L/\lambda_d) - 2\exp(-2\pi L/\lambda_d)\cos(2\pi L/\lambda_{osc})\} \qquad (16)$$

The value of $P_{\nu_\mu\nu_\tau}$ integrated over the energy and the zenith angle, for $\alpha = 0.3 \times 10^{-5} eV^2$ (the best fit for scenario (b)) is 0.33 for sub-GeV and 0.26 for multi-GeV. For $\alpha = 0.44 \times 10^{-3} eV^2$ (the second minima in the $\Delta\chi^2$ vs. α curve) the corresponding numbers are 0.21 and 0.15, while for the only $\nu_\mu - \nu_\tau$ oscillation case, the corresponding values are 0.37 and 0.26 respectively. The value of Δm^2 and $\sin^2 2\theta$ for both the cases is $0.003 eV^2$ and 1.0 respectively.

The fig. 9 shows that the zenith angle dependence of the scenario (b) is almost similar to the case of $\nu_\mu - \nu_\tau$ oscillation. But the two cases are very different in principle. For the oscillation case a larger θ implies a larger conversion whereas in scenario (b) a larger θ means the fraction of the unstable component is less in ν_μ and the depletion is less. If one compares the conversion probability as given by eq.(16) with the one for the $\nu_\mu - \nu_\tau$ oscillation case, then the scenario (b) considered in this paper would have smaller number of ν_τs in the resultant flux at the detector, especially for the larger values of α which are still allowed by the data and the two cases might be distinguished when one has enough statistics to detect τ appearance in Super-Kamiokande [19] or from neutral current events [20].

In our paper we have followed the procedure of data fitting as done in [7]. Thus we use the ratios for which the common systematic errors get canceled out. Strictly speaking one should use the absolute number of events and include all the correlations between bins and e-like and μ-like events. But the best-fit points and the allowed regions are not expected to change significantly [8]. We have compared the scenarios of neutrino oscillation and decay with the same definition of χ^2 and

for this purpose of comparison neglecting the correlation matrix will not make much difference. Apart from the statistical analysis we have given plots of R and Y for various values of the parameters. The allowed parameter ranges from these plots are consistent with what we get from our statistical analysis. The histograms that we have plotted are also independent of our definition of χ^2. We have checked that if we estimate the allowed ranges from the histograms these are consistent with what we get from our definition of χ^2. Thus we agree with the observation in ref. [7] that although this method of data fitting is approximate it works well. In our analysis we have used only the SK data because it has the highest statistics as compared to the earlier atmospheric neutrino experiments.

Radiative decays of neutrinos are severely constrained [21] and what we consider here are the non-radiative decay modes of the neutrino. Models for neutrino decay for the scenario (a) are discussed in [4, 22]. For the scenario (b) the unstable state decays to a sterile neutrino state and a light scalar. The model described in [23] in connection to the solar neutrino problem can be adapted to emulate this scenario. A recent paper [24] has discussed how such a model can be constructed. Since in scenario (b) the decay products are invisible there are no distinctive signs of the decay. Decay of leptons to the light scalar are prohibited from conservation of lepton number. Hence it is difficult to constrain these from laboratory experiments [23]. Consequences of such a model for astrophysics has been discussed in [24].

We would like to thank Anjan Joshipura for creating our interest in the neutrino decay solution to the atmospheric neutrino problem. We also like to thank Osamu Yasuda for many useful correspondences during the development of our computer code, S. Pakvasa for useful correspondences and Kamales Kar for discussion and encouragement. Finally we would like to thank Kate Scholberg for providing us with the 848 days data and for other useful correspondences.

References

[1] Y. Fukuda *et al.*, The Super-Kamiokande Collaboration, Phys. Lett. **B433** (1998) 9; Phys. Lett. **B436** (1998) 33; Phys. Rev. Lett. **81** (1998) 1562.

[2] M. Apollonio *et al.*, Phys. Lett. **B 420** (1998) 397.

[3] J.M. LoSecco, hep-ph/9809499; P. Lipari and M. Lusignoli, Phys. Rev. **D60** (1999) 0133003.

[4] V. Barger, J.G. Learned, S. Pakvasa and T.J. Weiler, Phys. Rev. Lett. **82** (1999) 2640.

[5] K. Scholberg, private communication.

[6] J.W. Flanagan, J.G. Learned and S. Pakvasa, Phys. Rev. **D57** (1998) 2649.

[7] R. Foot, R.R. Volkas and O. Yasuda, Phys. Rev. **D58** (1998) 013006.

[8] O. Yasuda, private communication.

[9] M. Honda, T. Kajita, S. Midorikawa, and K. Kasahara, Phys. Rev. **D52** (1995) 4985.

[10] T. K. Gaisser and J. S. O'Connell, Phys. Rev. **D34** (1986) 822.

[11] P. Lipari, M. Lusignoli and F. Sartogo, Phys. Rev. Lett. **74** (1995) 4384.

[12] M.C. Gonzalez-Garcia *et al.*, Phys. Rev. **D58** (1998) 033004; Nucl. Phys. **B543** (1999) 3.

[13] G.L. Fogli and E. Lisi, Phys. Rev. **D52** (1995) 2775.

[14] G.L. Fogli, E. Lisi, A. Marrone and G. Scioscia, Phys. Rev. **D59** (1998) 033001.

[15] The last one in ref [1].

[16] V. Barger, W.Y. Keung and S. Pakvasa, Phys. Rev. **D25** (1982) 907.

[17] See the corresponding figures of $\nu_\mu - \nu_\tau$ oscillations in [7].

[18] Our results for this hypothesis agrees well with that obtained in G.L. Fogli, E. Lisi, A. Marrone and G. Scioscia, Phys. Rev. **D59** (1999) 117303, although our data fitting procedures are different.

[19] L.J. Hall and H. Murayama, hep-ph/9810468.

[20] F. Vissani and A.Yu. Smirnov, Phys. Lett. **B432** (1998) 376.

[21] M. Fukugita, Phys. Rev. **D36** (1987) 3817.

[22] A. Acker, A. Joshipura and S. Pakvasa, Phys. Lett. **B285** (1992) 371.

[23] A. Acker, S. Pakvasa and J. Pantaleone, Phys. Rev. **D 43**, (1991) R1754, **D45** (1992) R1.

[24] V. Barger *et al.* hep-ph/9907421.

Figure Captions

Fig. 1. The allowed parameter region in Δm^2 -$\sin^2 2\theta$ plane for the $\nu_\mu - \nu_\tau$ oscillation hypothesis for the 848 days data. The solid line is the area allowed at 90% C.L. and the dashed line shows the area allowed at 99% C.L. The best-fit point is shown.

Fig. 2. The variation of R and Y with α for the sub-GeV neutrinos (denoted by the subscript sg) assuming neutrino decay with $\Delta m^2 > 0.1 eV^2$. The curves are drawn at fixed values of $\sin^2\theta$=0.03 (solid line), $\sin^2\theta$=0.04 (long dashed line), $\sin^2\theta$=0.06 (short dashed line), $\sin^2\theta$=0.08 (dotted line) and $\sin^2\theta$=0.1 (long dashed-dotted line). The short dashed-dotted lines give the SK 848 days results within a $\pm 1\sigma$ band. Also shown are the R and Y at the best-fit point.

Fig. 3. Same as in fig. 2 but for multi-GeV neutrinos.

Fig. 4. The variation of R and Y with Δm^2 for the sub-GeV neutrinos (denoted by the subscript sg) assuming neutrino decay with Δm^2 unconstrained. In these curves the α is fixed at it's best-fit value of $0.3 \times 10^{-5} eV^2$. The curves are drawn at fixed values of $\sin^2\theta$=0.7 (dotted line), $\sin^2\theta$=0.6 (short dashed line) and $\sin^2\theta$=0.5 (long dashed line). The solid lines give the curves for the best-fit value ($\sin^2\theta = 0.5$) of the $\nu_\mu - \nu_\tau$ oscillation case. The dotted-dashed lines give the SK 848 days results within a $\pm 1\sigma$ band. Also shown are the R and Y at the best-fit point.

Fig. 5. Same as in fig. 4 but for multi-GeV neutrinos.

Fig. 6. The $\Delta\chi^2 = \chi^2 - \chi^2_{\rm min}$ vs. α with Δm^2 and $\sin^2 2\theta$ unconstrained for the 848 days (solid line) and 535 days data (dotted line).

Fig. 7. The allowed parameter region for the 848 days data in the Δm^2 -$\sin^2 2\theta$ plane for 4 different values of α shown at the top of each panel. The solid and the dashed lines correspond to the area allowed at 90% C.L. and 99% C.L. respectively.

Fig. 8. The allowed parameter region for the 848 days data in the α-$\sin^2 2\theta$ plane for 4 different values of Δm^2 shown at the top of each panel. The solid and the dashed lines correspond to the area allowed at 90% C.L. and 99% C.L. respectively.

Fig. 9. The sub-GeV and multi-GeV μ event distributions vs. zenith angle for the various scenarios considered. N_μ is the number of μ events as given by eq. (3) and $N_{\mu 0}$ is the corresponding number with survival probability 1. The panels labelled SG(535) and MG(535) give the histograms for the sub-GeV and multi-GeV 535 days data respectively, while the SG(848) and MG(848) give the corresponding histograms for the 848 days data. For the both the sets the solid line corresponds to the best-fit $\nu_\mu - \nu_\tau$ oscillation solution, the long dashed line is for the best-fit for scenario (a) and the short dashed line for the best-fit for scenario (b). Also shown are the SK μ event distributions with $\pm 1\sigma$ error bars for both the sets.

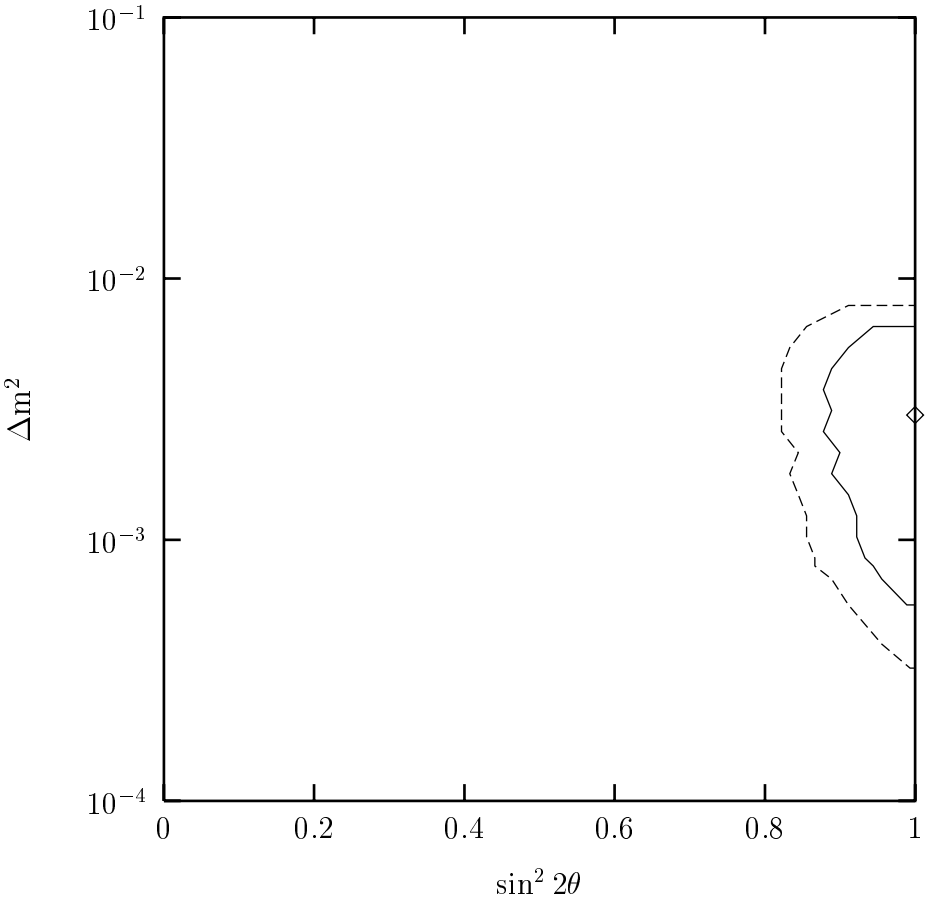

Fig. 1

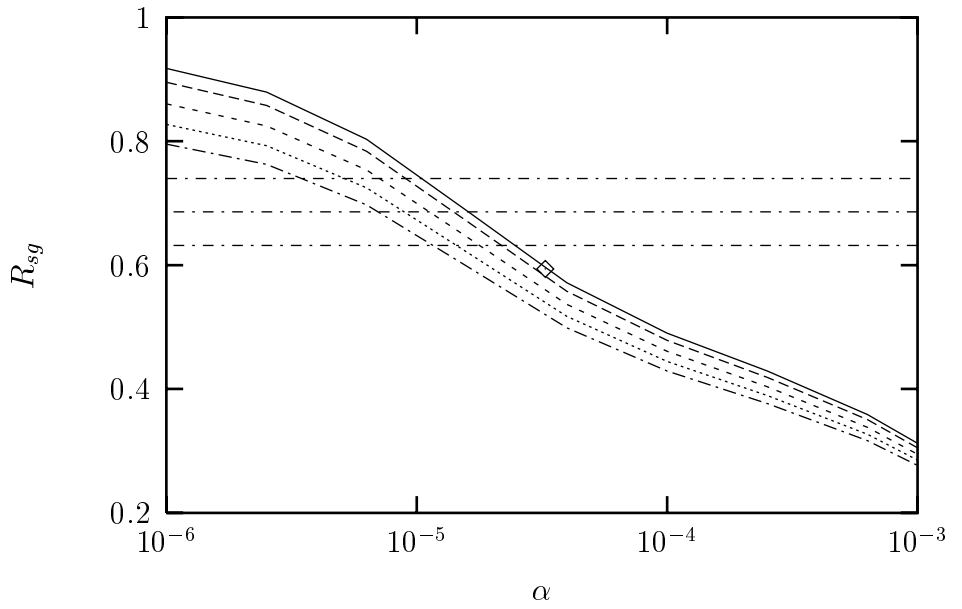
1
0.8
0.6
0.4
0.2
R_{sg}
10^{-6}
10^{-5}
10^{-4}
10^{-3}
α

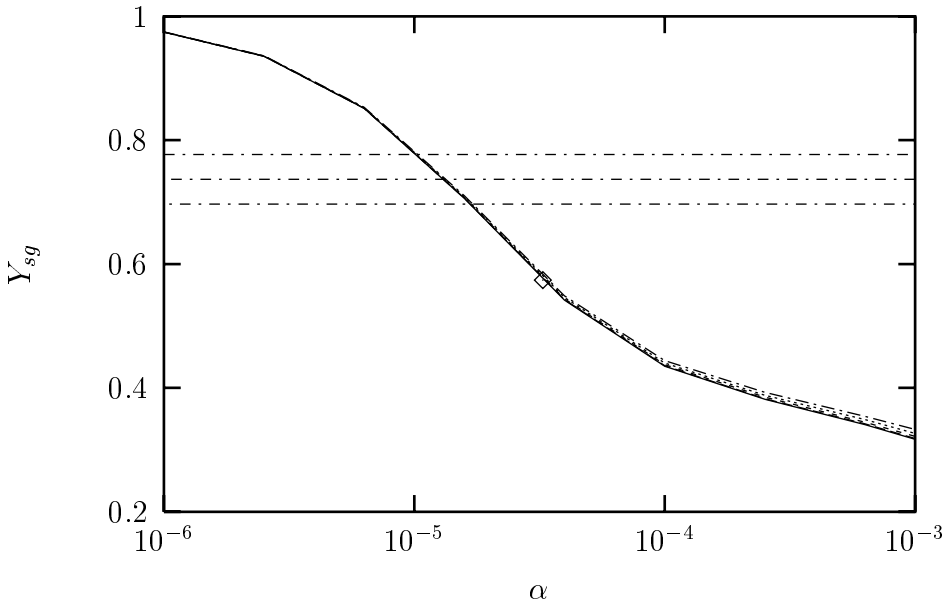
1
0.8
0.6
0.4
0.2
Y_{sg}
10^{-6}
10^{-5}
10^{-4}
10^{-3}
α

Fig. 2

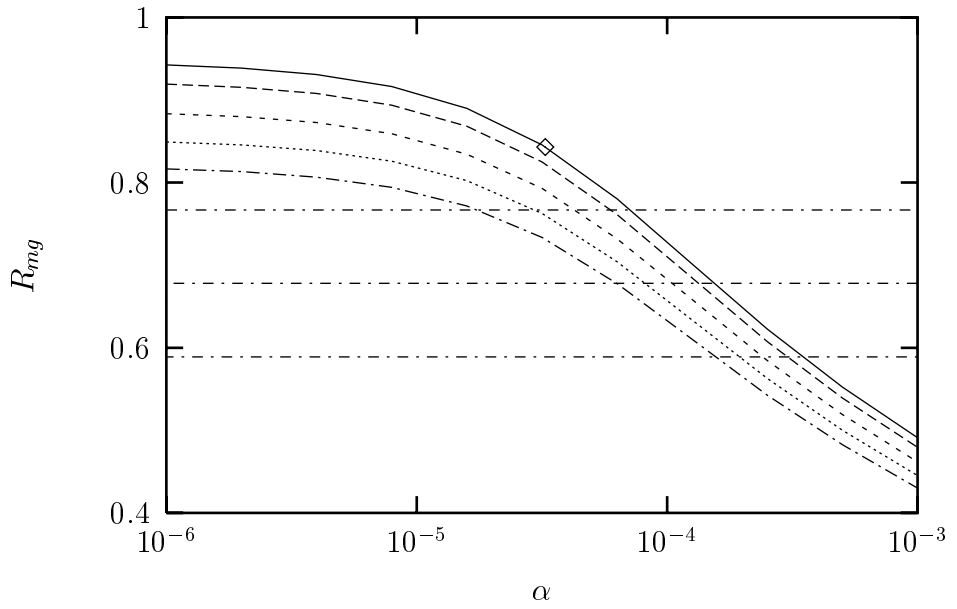
1
0.8
0.6
0.4
R_{mg}
10^{-6}
10^{-5}
10^{-4}
10^{-3}
α

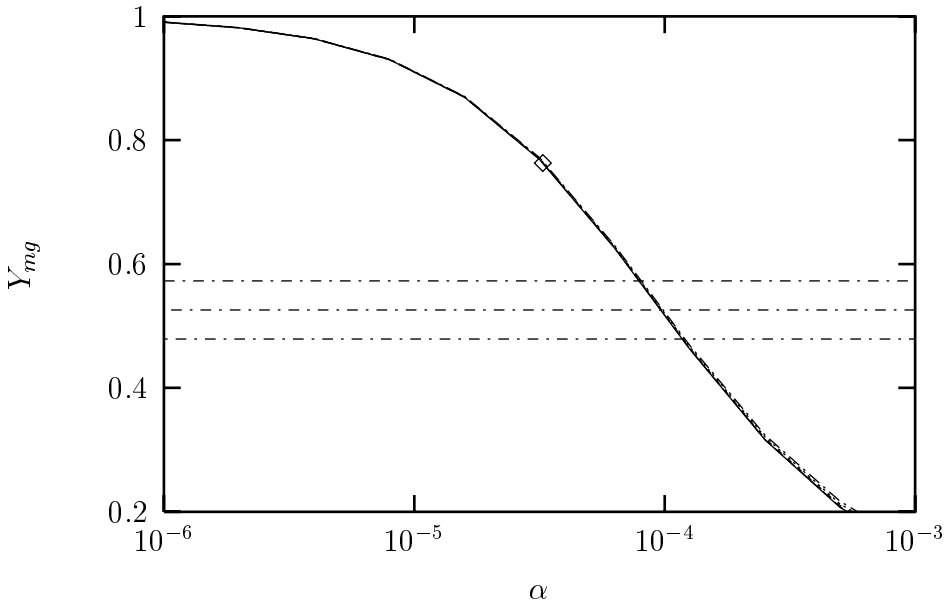
1
0.8
0.6
0.4
0.2
Y_{mg}
10^{-6}
10^{-5}
10^{-4}
10^{-3}
α

Fig. 3

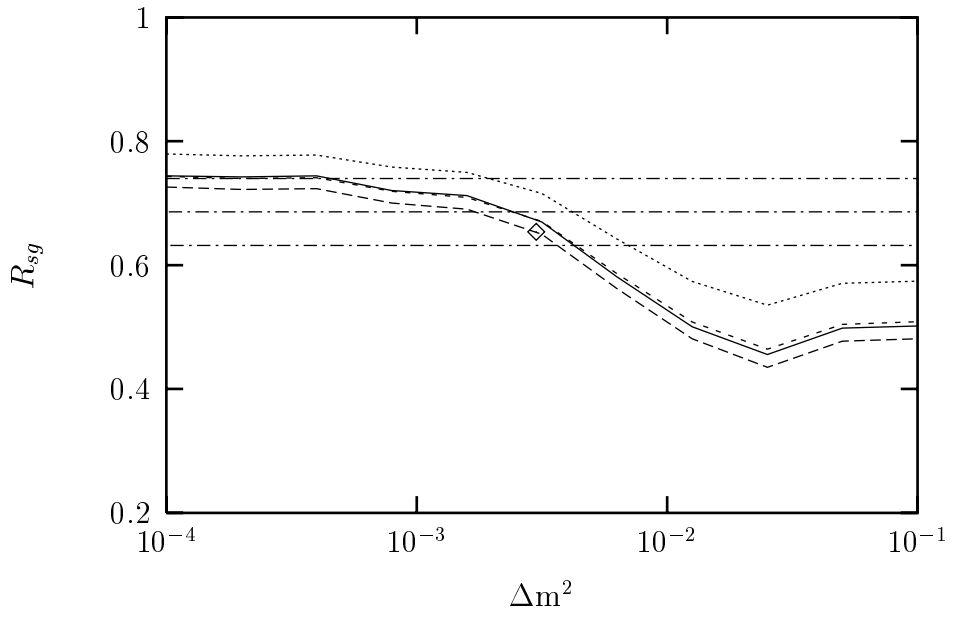
1
0.8
0.6
0.4
0.2
R_{sg}
10^{-4}
10^{-3}
10^{-2}
10^{-1}
Δm^2

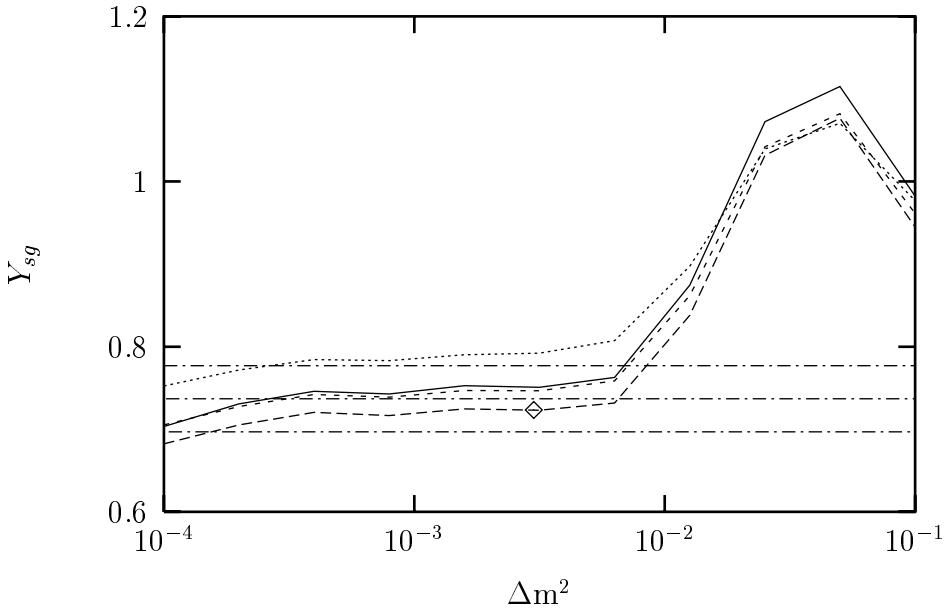
1.2
1
0.8
0.6
Y_{sg}
10^{-4}
10^{-3}
10^{-2}
10^{-1}
Δm^2

Fig. 4

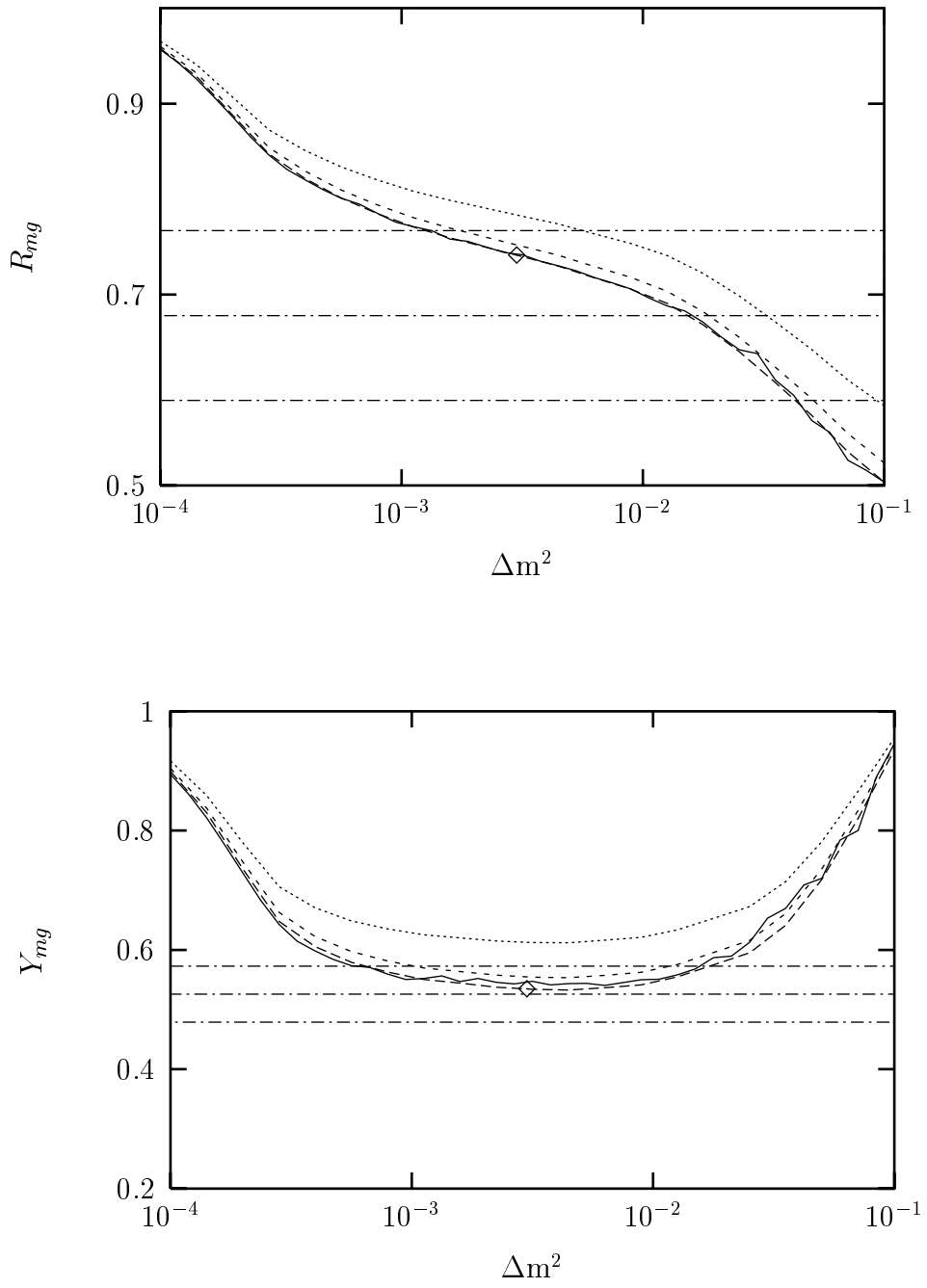
R_{mg}
0.9
0.7
0.5
10^{-4}
10^{-3}
10^{-2}
10^{-1}
Δm^2
Y_{mg}
1
0.8
0.6
0.4
0.2
10^{-4}
10^{-3}
10^{-2}
10^{-1}
Δm^2

Fig. 5

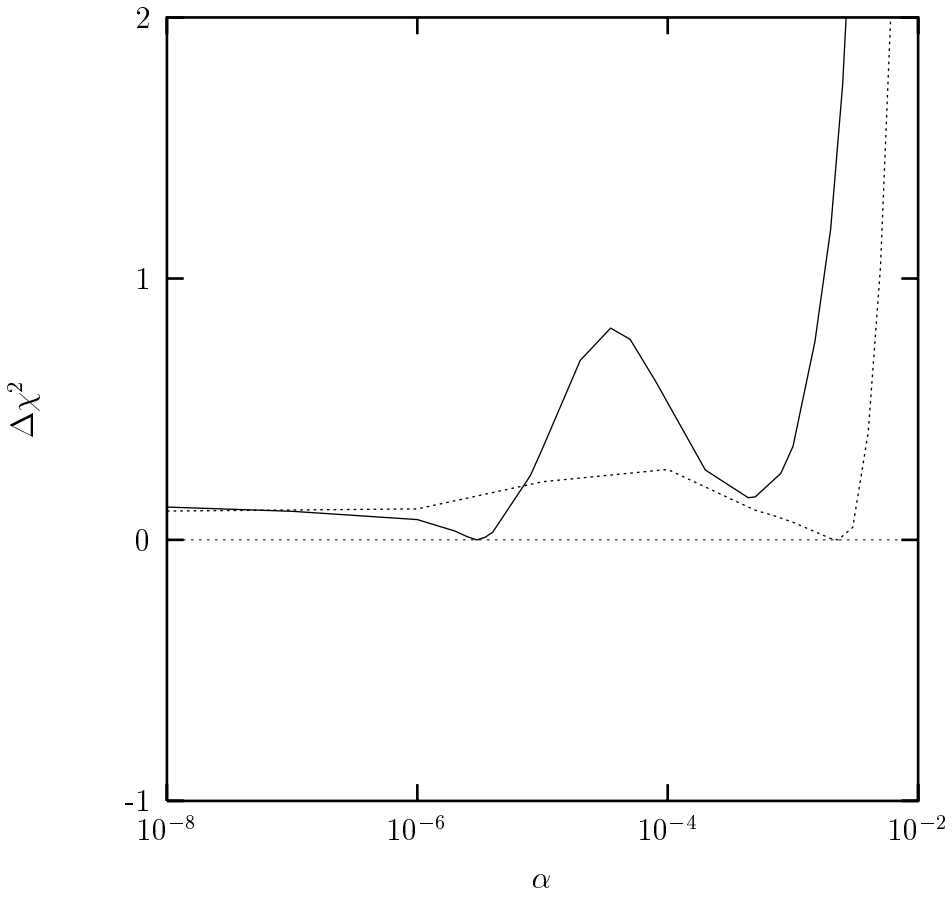

Fig. 6

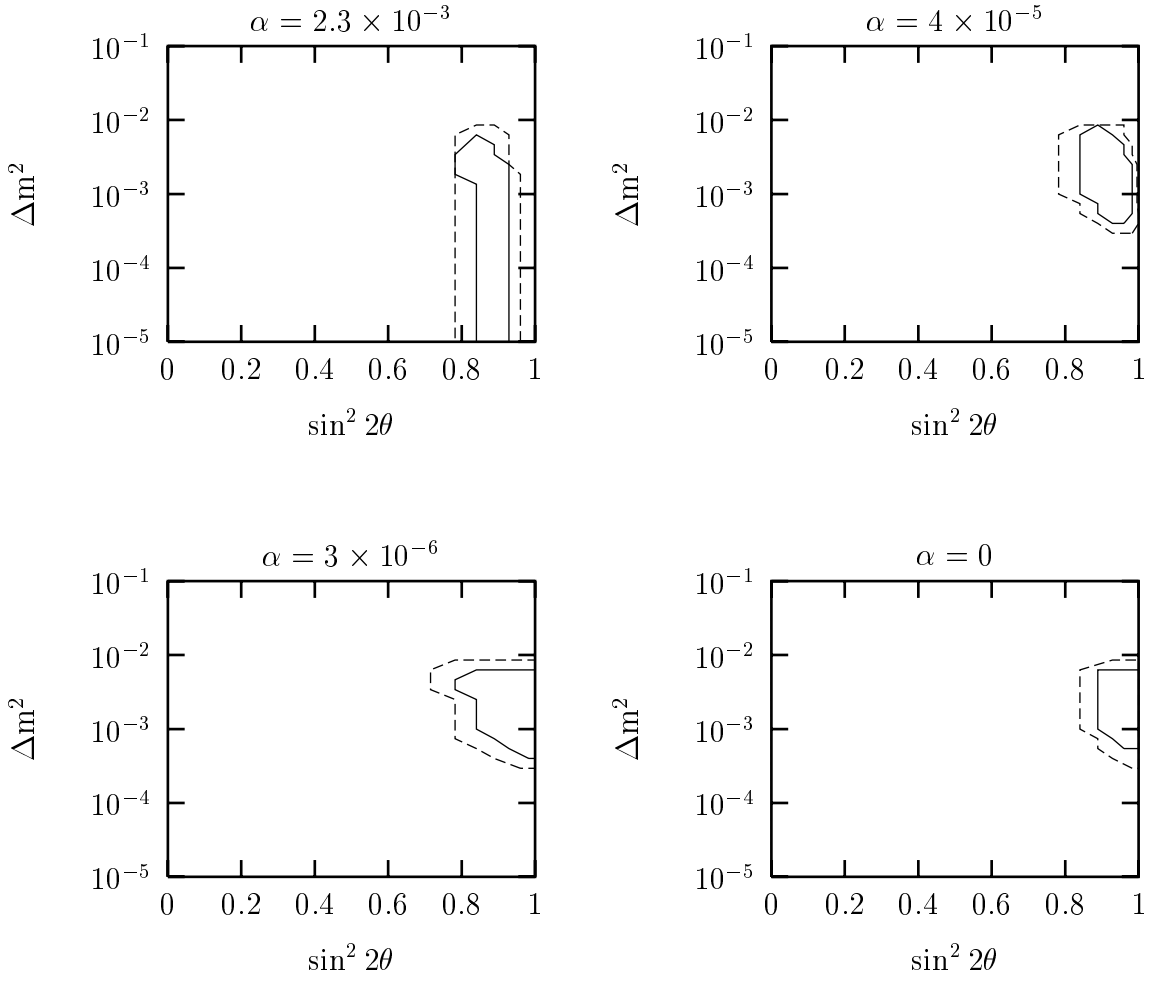
$\alpha = 2.3 \times 10^{-3}$
$\alpha = 4 \times 10^{-5}$
$\alpha = 3 \times 10^{-6}$
$\alpha = 0$
Δm^2
$\sin^2 2\theta$
10^{-1}
10^{-2}
10^{-3}
10^{-4}
10^{-5}
0
0.2
0.4
0.6
0.8
1

Fig. 7

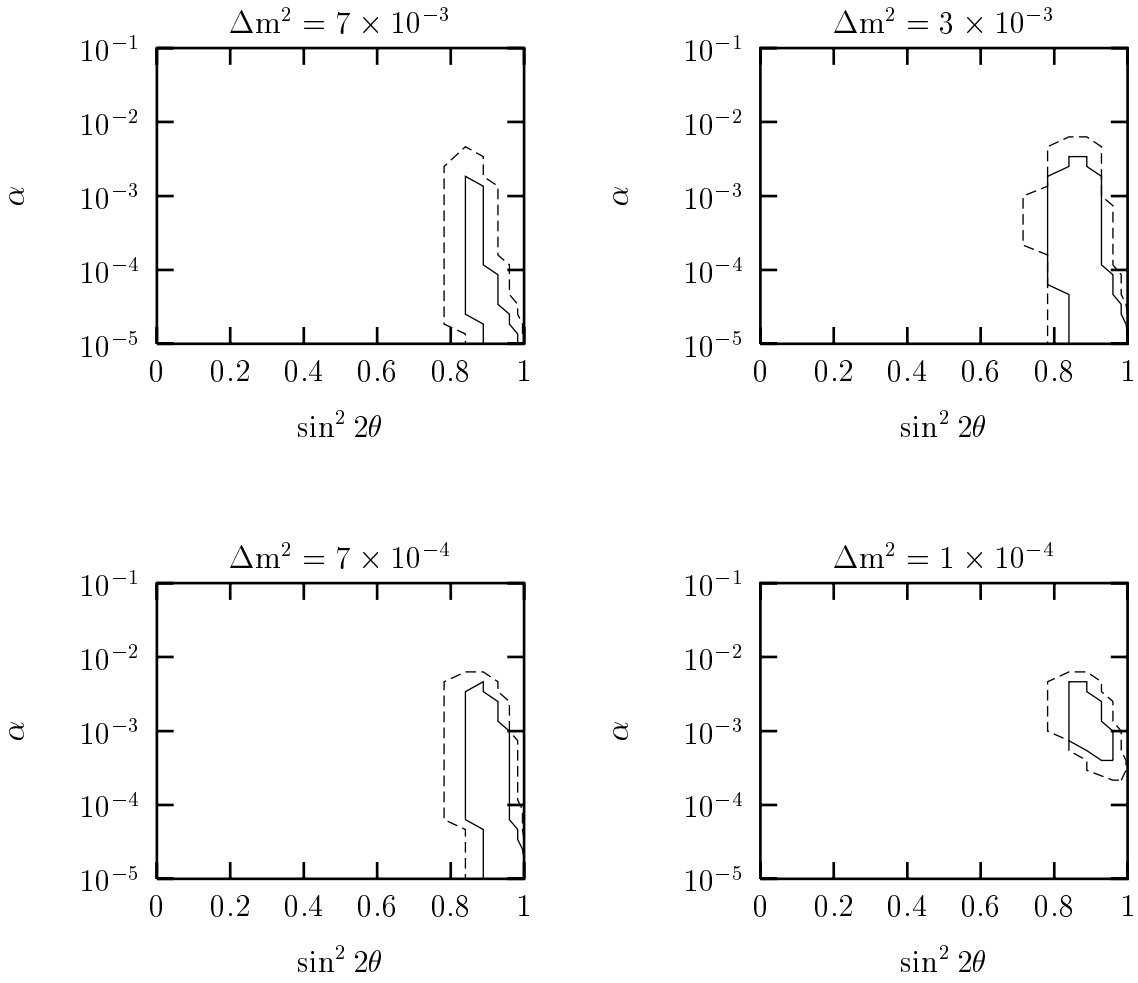
$\Delta m^2 = 7 \times 10^{-3}$
$\Delta m^2 = 3 \times 10^{-3}$
$\Delta m^2 = 7 \times 10^{-4}$
$\Delta m^2 = 1 \times 10^{-4}$
α
10^{-1}
10^{-2}
10^{-3}
10^{-4}
10^{-5}
0
0.2
0.4
0.6
0.8
1
$\sin^2 2\theta$

Fig. 8

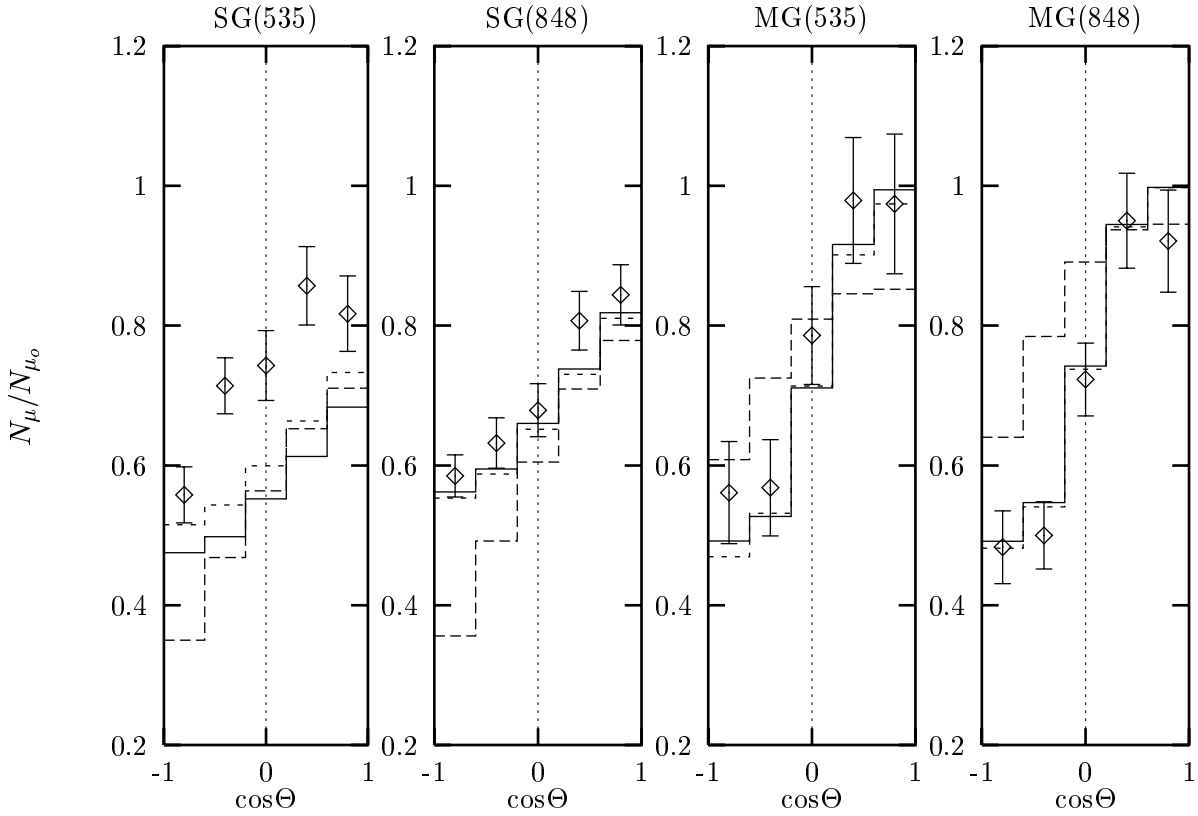

Fig. 9